

# Janus Colloidal Particles: Preparation, Properties, and Biomedical Applications

Chariya Kaewsaneha,<sup>†,‡</sup> Pramuan Tangboriboonrat,<sup>‡</sup> Duangporn Polpanich,<sup>§</sup> Mohamed Eissa,<sup>†,⊥</sup> and Abdelhamid Elaissari<sup>\*,†</sup>

<sup>†</sup>University of Lyon, F-69622, Lyon, France; University Lyon-1, Villeurbanne; CNRS, UMR 5007, LAGEP- CPE; 43 bd 11 Novembre 1918, F-69622 Villeurbanne, France

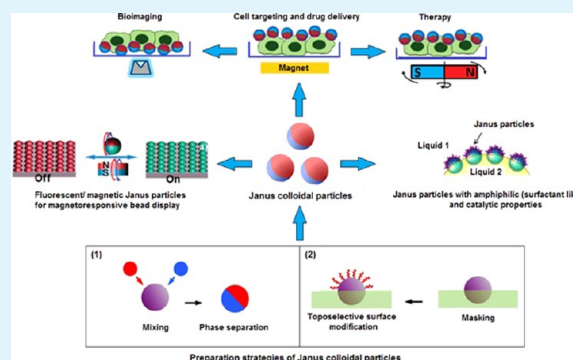
<sup>‡</sup>Department of Chemistry, Faculty of Science, Mahidol University, Phayathai, Bangkok 10400, Thailand

<sup>§</sup>National Nanotechnology Center (NANOTEC), Thailand Science Park, PathumThani 12120, Thailand

**ABSTRACT:** Janus or anisotropic colloidal particles comprising of at least two components of different chemistry, functionality, and/or polarity have attracted attentions in a wide range of applications, e.g., in optics, magnetics, plasmonics, colloidal chemistry, and biomedicine. The interesting features of Janus colloidal particles are attributed to their tunable and controllable asymmetric structure, which allows controlling their physicochemical properties, down to the nanoscale. Moreover, their synergistic potential for multiplexing, multilevel targeting, and combination therapies make them particularly attractive for biomedical applications. However, the synthesis of Janus colloidal particles must be well-adapted to get particles with precise control of their various structural/physical/chemical properties. Nowadays, the advance in new fabrication processes is a strong need for fabricating compact composite particles with spatially separated functionalities, uniform size, tunable composition, and effective response to stimuli.

In this review article, we summarized the most recent representative works on Janus colloidal particles including the various fabrication methods, important properties, and their potential applications, particularly in the biomedical field.

**KEYWORDS:** Janus, colloidal particles, synthesis, morphology, biomedical applications



## 1. INTRODUCTION

Nanoparticles play an important role in various biomedical applications as they can serve as superior optically stable bioimaging agents, and as solid support of biomolecules in immunoassay, and in biosensor devices for the early detection of diseases. In addition, they exhibit promising results in vitro and in vivo diagnostic and therapeutic purposes. In this regard, nanoparticles that express more than one functionality are often advantageous, which led to the synthesis of multifunctional nanostructures particles that combine various properties such as magnetism, photoluminescence, good colloidal stability, and biocompatibility. This in turn will enhance the detection of targeted biomolecules using multiple imaging techniques including magnetic resonance imaging (MRI) and fluorescence microscopy.<sup>1–5</sup>

In the past decade, anisotropic (Janus) particles with asymmetric geometry have attracted tremendous attention because of their fascinating properties including particular chemical composition, optical, magnetic, and surface properties such as charge or polarity. The term “Janus” was inspired from the Roman God Janus, with two heads placed back to back, looking to the future and past. This term was extended to encompass colloidal particles, which have different properties at

opposite sides.<sup>6,7</sup> Janus colloidal particles could be used as building blocks for supraparticular assemblies, as dual-functionalized devices, and as particular surfactants. The first report on Janus particles appeared in 1985 by Lee et al. who prepared asymmetric polystyrene (PS)/poly(methyl methacrylate) (PMMA) latex via seeded emulsion polymerization technique.<sup>8</sup> In the early 1991, P-G. de Gennes raised the concept of Janus particles in his Nobel Prize addressed. What de Gennes had in mind was that these amphiphilic Janus particles might behave like surfactant molecules to be adsorbed at the water–air interface, forming a monolayer as “skin that can breathe”, because small molecules would still be able to diffuse through the interstices between the Janus particles in the monolayer.<sup>9</sup>

In general, Janus colloidal particles can be divided into three main groups; polymer–polymer, inorganic–inorganic, and organic–inorganic hybrid particles. They might have spherical or nonspherical shape with various morphologies such as dumbbell-like, half-raspberry-like, acorn-like, snowman-like, and mushroom-like.<sup>10–12</sup> For the fabrication of Janus particles,

**Received:** October 31, 2012

**Accepted:** February 8, 2013

**Published:** February 8, 2013



**Figure 1.** (A) Schematic illustration of the preparation of Janus PAN/PS colloidal particles via the seeded emulsion polymerization of St in the presence of cross-linked PAN hollow seed, followed by PS bulge growth on seed particle and favorable growth of other materials, (B) Scanning electron microscopy (SEM) of Janus PAN/PS polymer colloidal particles (monomer/PAN seed weight ratio = 4:1 with the DVB/St weight ratio at 3:1). Reproduced with permission from ref 14. Copyright 2010 American Chemical Society.

several methods have been used involving emulsion polymerization (emulsion, seeded emulsion and/or miniemulsion polymerization, and Pickering emulsion method), selective surface modification, and photopolymerization in microfluidic devices. All these strategies are based on phase separation of the materials composition and toposelective surface modification methods.<sup>10,13</sup>

This review focuses on three main parts, including synthesis and formulation of Janus colloidal particles, properties, and their potential applications in the biomedical domain. The commonly explored routes, pioneering works, and recent published articles on these interesting particles are discussed in detail.

## 2. SYNTHESIS AND FORMULATION OF JANUS COLLOIDAL PARTICLES

To obtain multifunctional Janus colloidal particles (e.g., polymer–polymer, inorganic–inorganic, or organic–inorganic hybrid particles) with tunable morphological structure and physical/chemical properties, we need high-throughput and low-cost techniques. The commonly used methods for fabrication of the various types of Janus particles, and particularly Janus colloidal particles (Janus droplets) are described.

### 2.1. Polymer–Polymer Janus Colloidal Particles.

Several methods including emulsion polymerization and solvent evaporation method can be used for the preparation of Janus particles. Among many methods, emulsion polymerization is considered as the key step for the fabrication of polymer–polymer Janus particles and their formation under growth-seeded conditions. The synthesis of these particles via polymerization in dispersed media is based mainly on phase separation strategy whose principal involves swelling of a cross-linked seed particle by a monomer that is subsequently polymerized.<sup>14,15</sup> The resulting polymer is no longer soluble in the seed particle and aggregates from the template particle forming small bulbs on the surface of the seed particles. Several parameters, e.g., cross-linking degree of seed latex, rate of monomer feeding, and polymerization time, affect the size distribution and morphology of the particles. In the preparation of submicrometer Janus particles of polyacrylonitrile (PAN) and PS via the one-step batch seeded emulsion polymerization (Figure 1A), both the high degree of cross-linking and the slow feeding of monomer were crucial to control the resultant anisotropic structure.<sup>14</sup> Submicrometer cross-linked PAN hollow colloid was used as a seed, and the mixture of styrene/divinylbenzene (St/DVB) was slowly added into the seed latex followed by polymerization at high temperature. Since PAN and PS are typically immiscible, PS phase separated from the PAN shell driven by polymer network elastic-retractile force during cross-linking providing Janus PAN/PS polymer

colloids (Figure 1B). The polymerization-induced phase separation is mainly responsible for the growth of Janus colloidal particles and the slow monomer feeding is important to achieve the small anisotropic colloids. In addition, sufficient cross-linking of the formed polymer is required to enforce a complete phase separation. By favorable growth of other materials therein, Janus inorganic/polymer composite colloids were also synthesized. Similarly, Janus particles of the soft poly(*n*-butyl acrylate) (PnBA) and the hard PMMA with a diameter of 132 nm were synthesized by swelling of MMA monomer through PnBA seed before polymerization.<sup>15</sup> Transmission electron microscope (TEM) images clearly showed the phase-separation leading to hemisphere-like structure of particles predominated by the impact of the thermodynamic factor.

Besides the seeded emulsion polymerization technique, the internal phase separation accompanied by solvent evaporation technique was utilized to produce polymer–polymer Janus colloidal particles in a large scale.<sup>16–18</sup> In this process, the polymer is dissolved in a mixture of volatile and nonvolatile solvents. In this case, a sufficient volume of a good solvent is required to ensure complete solubility of the polymer. The polymer solution is subsequently dispersed in a water/emulsifier mixture to produce an oil-in-water emulsion, followed by evaporation of the volatile solvent. This in turn leads to a change in the droplets composition, and finally the polymer-rich phase separates as small droplets within the emulsion droplet. The polymer-rich droplets then migrate to the oil/water interface, where they coalesce to form polymer particles. In the preparation of PMMA and PS particles with Janus-like morphology via the internal phase separation followed by extraction of the oil template, the emulsified polymer/hexadecane/CH<sub>2</sub>Cl<sub>2</sub> droplets in aqueous solution were first prepared.<sup>16</sup> Then, the internal phase separation was triggered by evaporation of CH<sub>2</sub>Cl<sub>2</sub> from the emulsion droplets, which led to the formation of PMMA/PS/hexadecane particles. Finally, the extraction of hexadecane led to the formation of PMMA/PS colloidal particles with different morphologies (ball in bowl and/or capped sphere) which were highly affected by the ratio of the two polymers. By using PS/PMMA at weight ratio 75/25, the small caps particle morphology was obtained. More interestingly, by decreasing PS/PMMA ratio to 50/50 and 33/67, a ball in bowl morphology was observed. Similarly, micrometer-size and monodisperse particles of PMMA and poly(styrene-2-(2-bromoiso-butyl)oxy)ethyl methacrylate) (P(S-BIEM)) composite particles with mushroom-like morphology were also synthesized based on the internal phase separation (Figure 2A).<sup>17</sup> The formation of hemisphere of PMMA and P(S-BIEM) was introduced by solvent evaporation of toluene from toluene droplets containing the dissolved two polymers, which dispersed in aqueous solution. The site

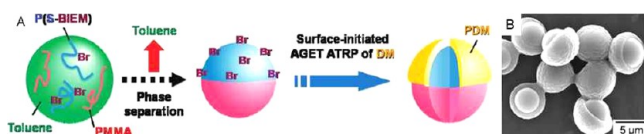


**Figure 2.** (A) Schematic illustration for fabrication of mushroomlike morphology of PMMA/P(S-BIEM-g-PDM) Janus colloidal particles by the site selective surface-initiated ATRP of DM in an aqueous medium using biphasic Br groups at one side of the homogeneous PMMA/P(S-BIEM) surface as macroinitiator, (B) SEM photograph of PMMA/P(S-BIEM-g-PDM) Janus colloidal particles. Reproduced with permission from ref 17 Copyright 2010 American Chemical Society.

selective surface-initiated atom transfer radical polymerization (ATRP) of 2-(dimethylamino) ethyl methacrylate (DM) was subsequently carried out on one side of the surface of hemispherical PMMA/P(S-BIEM) composite particles in an aqueous dispersed system using biphasic Br groups as macroinitiator. After polymerization, the morphology of the particles changed from spherical to mushroom-like shape (Figure 2B). The mushroom-like morphology of PS and poly[methyl methacrylate-(chloromethyl) styrene] [P(MMA-CMS)] composite particles was also prepared by this method.<sup>18</sup>

## 2.2. Inorganic–Inorganic Janus Colloidal Particles.

Inorganic–inorganic Janus colloidal particles can be divided into two types; a pair of two different inorganic materials, and a single inorganic particle with different chemical composition and/or properties on both sides. In general, the fabrication of the first type is based on the controlled nucleation and growth of a single particle onto the surface of a precursor which provides various shapes, e.g., dumbbell-like, snowman-like or acorn-like morphology.<sup>19</sup> In this context, the uniform heterodimer nanoparticles of FePt–Au bearing multifunctionality were successfully fabricated by prevention of the nucleation of isolated Au onto the surface of FePt.<sup>20</sup> The FePt nanoparticles were allowed to react with AuCl(PPh<sub>3</sub>) in 1,2-dichlorobenzene containing 1-hexadecylamine under inert atmosphere of H<sub>2</sub>/Ar mixture. The Pt containing nanoparticle seeds served as a catalytic surface for reduction of gold ions (Au<sup>+</sup>) to metallic gold (Au<sup>0</sup>). Then, the successive growth of Au to the seed resulted in heterodimers of FePt–Au (Figure 3A). In the other work, asymmetric silica–Au particles were fabricated by dewetting half-shells of Au deposited on the surface of spherical silica colloidal particles.<sup>21</sup> At first, an adhesive layer of Ti/W alloy was sputter coated onto a half of

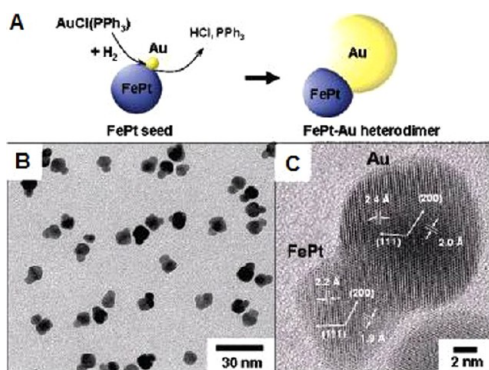


**Figure 3.** (A) Schematic route of FePt–Au heterodimer formation, (B) TEM, and (C) high-resolution (HR)-TEM image of FePt–Au heterodimer particles. Reproduced with permission from ref 20. Copyright 2006 American Chemical Society.

the silica surface that placed on a silicon wafer, followed by another thin layer of Au. After annealing, the mobility of Au half-shell beaded up by dewetting from its edge where it was the thinnest. Each Au half-shell was then transformed into a microcrystal formed via this process. By controlling the size of Au microcrystals, it was possible to limit the number of molecules that further immobilized on the surface of each dimeric particle. The dumbbell-like bifunctional composite nanoparticles of Au–Fe<sub>3</sub>O<sub>4</sub> were prepared via the decomposition of Fe(CO)<sub>5</sub> over the surface of the preformed Au nanoparticles, followed by oxidation in air.<sup>22</sup> The dumbbell structure was formed through epitaxial growth of iron oxide on the Au seed which was affected by the polarity of the solvent, as in the case of using diphenyl ether. Similarly, the dumbbell-like morphology of Ag–Fe<sub>3</sub>O<sub>4</sub> was prepared by growing Ag nanoparticles onto Fe<sub>3</sub>O<sub>4</sub> seed particles.<sup>23</sup>

The method based on toposselective surface modification strategy has been also used for fabrication of inorganic–inorganic Janus particles. In this strategy, partial coverage of the inorganic particles surface is required, followed by functionalization of the remaining surface by the chemical modification or by using other inorganic particles. Asymmetric Janus silica particles with diameter of 450 nm were fabricated by the sequential arranged particle-embedding and surface-modification process.<sup>24</sup> Only one side of the particles was embedded into polymer–fiber substrates by thermal process and the other side surface was subsequently modified by silanization. Janus particles with two hemispherical surfaces, one-half comprising of raw silica and the other half consists of amino-functionalized surface, were produced. Thermal manipulation of the embedded particles allowed the following silanization modifications to be restricted only to the exposed two-thirds, half, or one-third silica surfaces. After labeling of the amino-enriched surface with Au nanoparticles, the Janus particles with distinguished functionalized hemispheres at the desired ratios were obtained (Figure 4A). To prepare bifunctionalized Janus particles, the sphere surfaces were labeled with Au nanoparticles prior to adsorption of silica particles onto the fiber surfaces. The exposed surface was then etched with a basic solution and subsequently relabeled with citrate-modified Fe<sub>3</sub>O<sub>4</sub> nanoparticles. In addition, ternary Janus particles were designed. The one-third-embedded silica particles were first treated with silane via chemical-vapor-deposition (CVD) process and then labeled with Au nanoparticles. The temperature was increased for the supplementary embedding that buried the particle midsection and protected it from chemical or physical modification. The remaining one-third-exposed hemisphere was then etched with a basic solution to remove the aminosilane moieties and Au nanoparticles from the silica surface.

Moreover, the inorganic–inorganic Janus particles with controllable chemical patchiness and anisotropic structure with different properties, e.g., color coding, and recognition properties, have been demonstrated by using this method.<sup>25</sup> For instance, PMMA layer was spin-coated onto a monolayer of silica particles (5 μm), which monodeposited on substrate. By subjecting the formed particles to O<sub>2</sub> plasma etching for 5–90 s, various sizes were generated on the particle surfaces with chemical patchiness. After removal of PMMA layer by organic solvent, monofunctionalized Janus particles were formed. Upon removal of the remaining PMMA layer, a second chemical functionalization could be performed to form bifunctionalized Janus particles. Furthermore, the asymmetric chemical



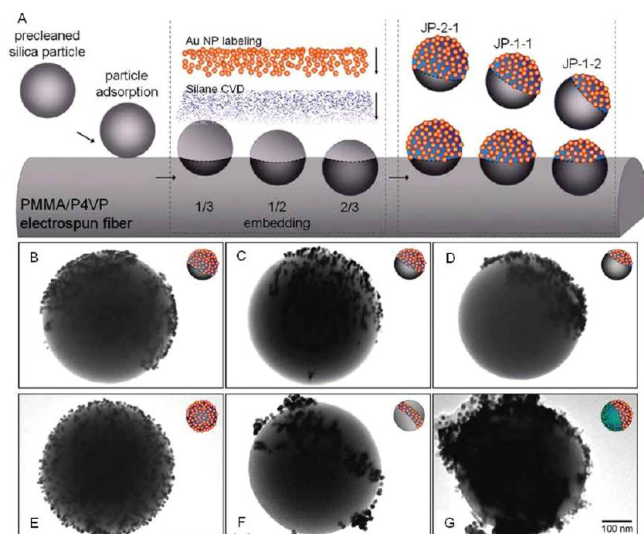


**Figure 4.** (A) Schematic representation of the fabrication of silanized silica particles labeled with Au nanoparticles; the ratio of Au particles was inversely proportional to the depth of silica embedded in polymer-fiber; 1/3, 1/2, and 2/3 refer to JP-2-1, JP-1-1, and JP-1-2, respectively. (B–G) TEM images of JP-2-1, JP-1-1, JP-1-2, a fully silanized silica particle labeled with Au nanoparticles, a ternary particle, and bifunctionalized Janus particle, respectively. Reproduced with permission from ref 24. Copyright 2010 American Chemical Society.

functionality of the particles would be further employed for coupling with secondary molecules or nanoparticles, forming anisotropic particle structure. Then, Janus particle or

anisotropic particle structure was released from the surface by sonicating the substrate in water.

**2.3. Organic–Inorganic Colloidal Particles.** The organic–inorganic or polymer–inorganic Janus colloidal particles can also be prepared via the seeded emulsion polymerization. Although this route is derived from the growth-seeded emulsion polymerization technique; the seeds are mainly composed of inorganic particles. During polymerization process, several parameters, e.g., inorganic and polymer content, polymer composition, type and amount of initiators used, must be adapted. In this context, Elaissari et al. prepared magnetic PS-DVB latex particles using emulsion polymerization of St and DVB monomers in the presence of preformed oil-in-water (O/W) magnetic emulsion droplets as seeds.<sup>26</sup> The key parameters, including type of magnetic emulsion, St/DVB monomers ratio, DVB amount, type of initiator and surfactant nature, affecting the formation and morphology of the prepared magnetic latexes were investigated. Both low and high octane content magnetic emulsions stabilized by different types of surfactants including ammonium persulfate (AP), poly-(oxyethylene) isooctylphenylether (Triton X-405) and sodium dodecyl sulfate (SDS), were used. In addition, four different initiators, i.e., 2,2'-azobis(2-methylpropionitrile) (AIBN), 2,2'-azobis(2-methylpropionamide) dihydrochloride (V50), 4,4'-azobis(4-cyanopentanoic acid) (ACPA), and potassium persulfate (KPS), were examined. It was found that the morphology (Janus-like, moon-like, and/or core-shell) of the prepared magnetic latex particles depended mainly on the used formulation (Figure 5). For instance, the polymerization of St monomer in presence of the oil-soluble AIBN initiator led to the formation of anisotropic morphology, whereas the

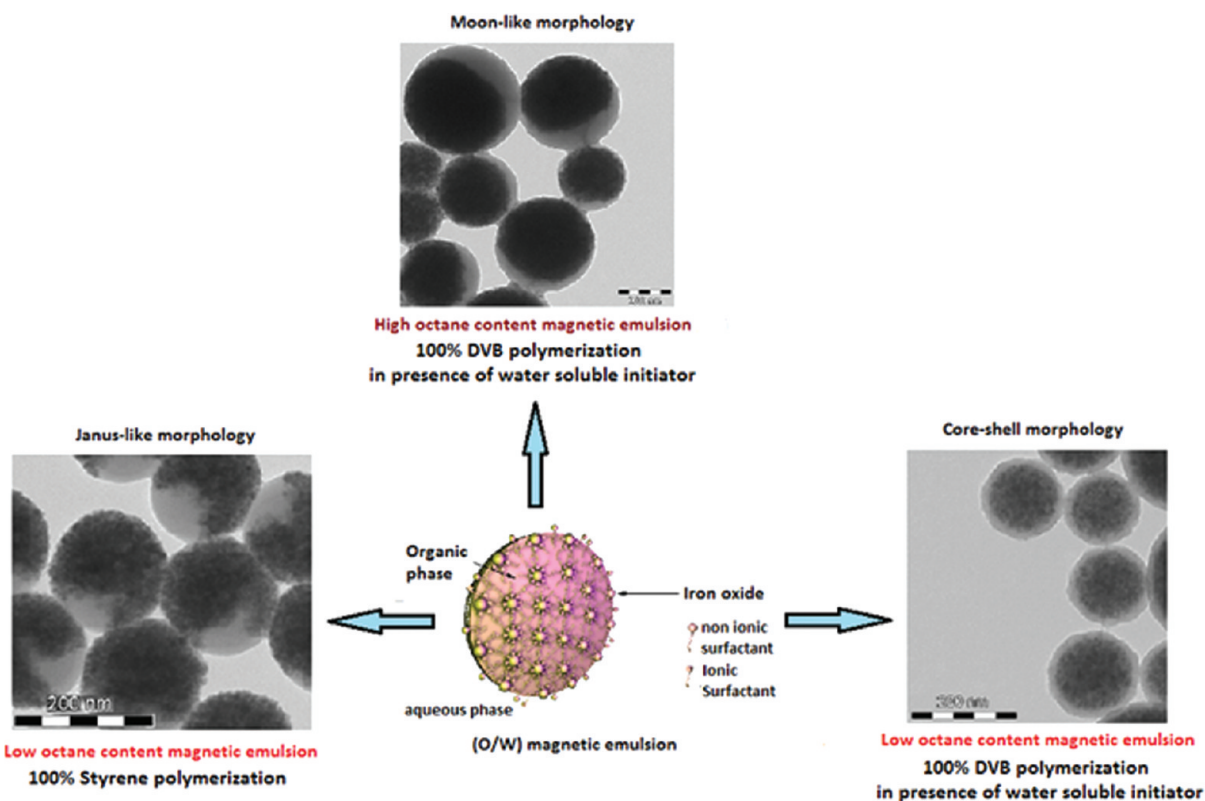


**Figure 5.** Morphology control of (O/W) magnetic emulsion used as seed in emulsion polymerization of St and DVB. The use of appropriate recipe leads to Janus, moonlike or magnetic core–polymer shell morphology. Adapted with permission from ref 26. Copyright 2013 Springer-Verlag.

progressive addition of DVB in presence of the water-soluble initiator (KPS) caused the formation of a well-defined magnetic core and polymer shell structure.

Similarly, Janus magnetic PS hybrid microparticles were also obtained via emulsion and/or miniemulsion polymerization of St using AIBN initiator at a proper ratio and magnetic emulsion as seed.<sup>27,28</sup> The hemisphere morphology or Janus particles obtained was a result of the thermodynamic incompatibility between PS and magnetic core of the ferrofluid droplet. Although a large amount of cross-linker DVB was participated, the final particle morphology did not show any significant improvement (Figure 6).<sup>27</sup> With KPS, homogeneous magnetic

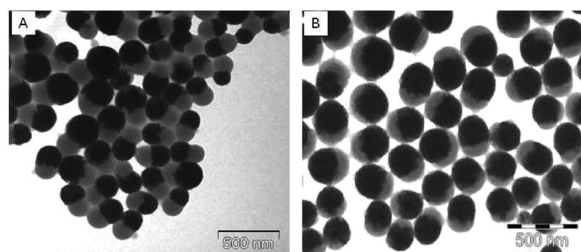


**Figure 6.** Magnetic polymeric Janus nanoparticles using AIBN as initiator (A) with and (B) without DVB. Adapted with permission from 27. Copyright 2011 John Wiley and Sons.

nanoparticles embedded in PS sphere as core-shell was obtained. This was attributed to the existence of sulfate groups, derived from KPS, on the surface of magnetic nanoparticles which enhanced the affinity of polymer matrix and water phase and allowed the polymeric phase to remain outside the particle forming core-shell morphology.

Furthermore,  $\text{Fe}_3\text{O}_4$ -PS Janus colloids of silica-coated  $\text{Fe}_3\text{O}_4$  eccentrically located at the one end of PS matrix were obtained via the seeded emulsion polymerization by changing the monomer/polymer swelling ratio.<sup>29</sup> At the early stage of polymerization, the particles of silica-coated  $\text{Fe}_3\text{O}_4$  surrounded with PS/DVB shell had spherical and concentric morphology due to low concentration of the starting monomers. As the thickness of PS/DVB polymer shell increased, more St monomer was absorbed by the cross-linked polymer networks. In the final stage, the elastic stress driven by the entropy change

of the swollen networks caused phase separation of the monomer from the network and eventually formed additional bulges attached to the original particles. Various morphologies, e.g., dumbbell-like or snowman-like particles of silica-PS, were also obtained via the seeded emulsion polymerization by controlling the ratio of the number of silica seeds to the number of growing nodules of PS.<sup>30</sup> The silica surface was modified by grafting with methacrylate groups, which promoted the fast polymerization of St monomer or oligomers directly onto the silica surface. When the number of silica spheres was close to that of PS nodules synthesized in situ, asymmetrical structures associated with each silica sphere to a single nodule were obtained.

In the past decade, miniemulsion polymerization technique is considered as one of the most effective methods for incorporating inorganic particles into polymer matrix. Miniemulsion is typically obtained by ultrasonication a system containing water, surfactant, monomer, costabilizer, and initiator. Both the particle nucleation and the subsequent propagation reaction occur primarily in submicrometer monomer droplets which considered as individual nano-reactors. The droplet size (50–500 nm) is adjusted by the type and amount of surfactant and costabilizer, the volume fraction of the disperse phase, and the homogenization process. For preparation of polymer-inorganic Janus colloidal particles, the encapsulated inorganic material is dispersed in an organic or monomer phase prior to miniemulsification. In most cases, the elastic stress driven by the entropy change in the swollen network can cause phase separation during polymerization at elevated temperature resulting in two-phase nonspherical particles. For instance, asymmetric nanocomposite particles pairs of silica and PS were obtained by combination of miniemulsion polymerization and the local modification of silica seed nanoparticles.<sup>31,32</sup> The surface of monodispersed silica particles, with 120 nm diameter, was partially modified with n-octadecyltrimethoxysilane (ODMS) to exhibit hydrophobicity, while the rest of their surface remained hydrophilic (Figure 7A). These particles were mixed with St monomer and aqueous solution of surfactant before ultrasonication. Asymmetric compound droplets with monomer droplets partially linked on the silica surface were formed due to the strong hydrophobic interaction between monomer molecules and the

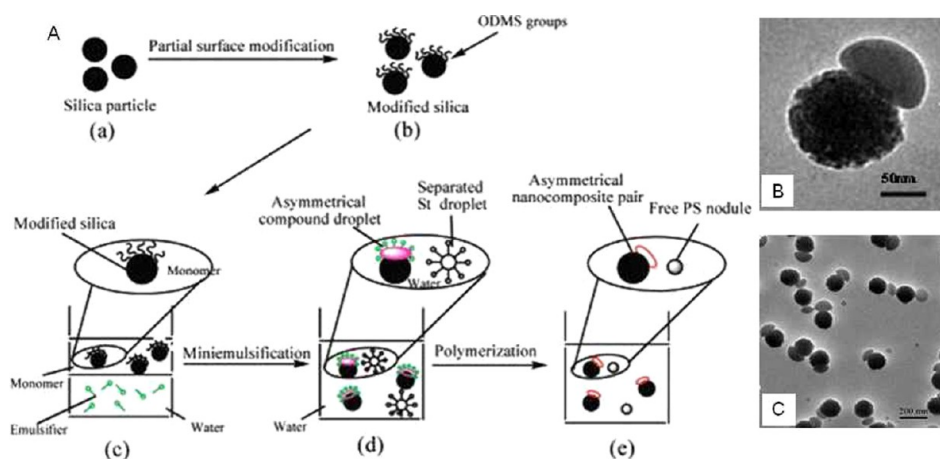


**Figure 7.** (A) Synthesis strategy in miniemulsion polymerization based on asymmetric modified silica particles, and TEM images of mushroom-like structure of silica/PS nanocomposite particles: (B) single pair and (C) multi pairs. Reproduced with permission from ref<sup>31</sup>. Copyright 2008 American Chemical Society.

modified area of silica surface. After polymerization, highly asymmetric nanocomposite particle pairs were obtained (Figure 7B). This strategy could be adapted to synthesize anisotropic silica-PS particles with several morphologies, e.g., mushroom-like, hollow egg-like and bowl-like structure, by controlling the weight ratio of the monomer/silica particles.<sup>32</sup>

However, the preparation of asymmetric particles via the miniemulsion polymerization is template-assisted; at least three steps, including template preparation, template modification, and asymmetric particle preparation, are indispensable. Another interesting method was used for the synthesis of silica-PS hybrid nanoparticles in one step.<sup>33</sup> Briefly, a mixture of St monomer, silane couple ( $\gamma$ -methacryloxypropyltrimethoxysilane; MPS), and inorganic precursor (tetraethoxysilane; TEOS) were directly confined in miniemulsion microreactor droplets, and each pair of organic and inorganic particles were simultaneously formed in one microreactor (Figure 8A).

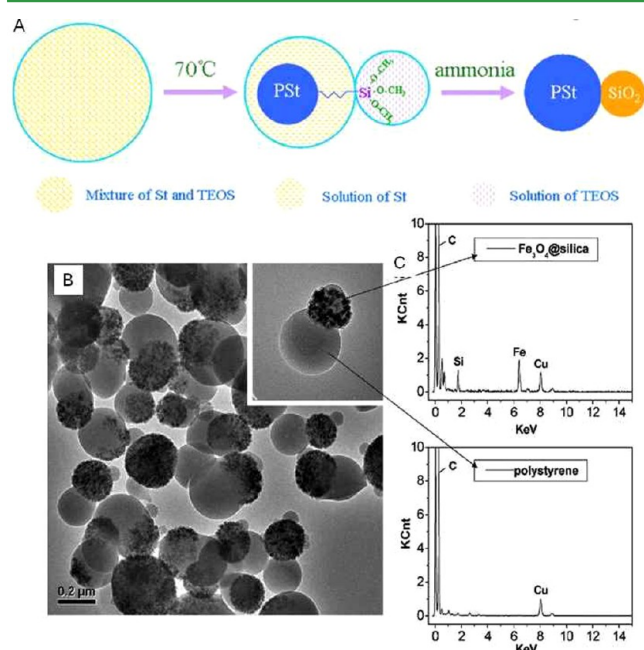


**Figure 8.** (A) Schematic diagram of the one-step synthesis of PS-silica Janus particles via miniemulsion polymerization technique. Reproduced with permission.<sup>33</sup> Copyright 2008. Elsevier. (B) TEM image of asymmetric Fe<sub>3</sub>O<sub>4</sub>/silica/PS composite particles and (C) Energy-dispersive X-ray (EDX) analysis of the as-synthesized asymmetric magnetic composite particles shown in the inset of B. Reproduced with permission from ref 35. Copyright 2011 American Chemical Society.

After polymerization of St, the phase separation of TEOS nodules from the initially formed PS particles occurred. The residual chain of MPS copolymerized onto PS particles would give birth to migration and be rich in TEOS liquid bulbs and caught hold of silica particles via copolycondensation with TEOS. After adding ammonia, the hydrolysis and polycondensation of TEOS and MPS could be accelerated and the phase separation between PS and silica was enhanced due to the hydrophobicity of PS and the hydrophilicity of silica. By using this method, neither the preparation of template particles in advance nor the complicated modification of the templates was necessary. Moreover, the size of PS particles in asymmetric dimer particles was easily adjusted by changing either the weight ratio of St/TEOS or the sonication power during the

miniemulsion preparation. This facile one-pot method was also adapted to synthesize asymmetric magnetic composite nanoparticles of iron oxide, silica, and PS.<sup>34,35</sup> When magnetic particles were dispersed in the mixture of monomers before polymerization, asymmetric magnetic Janus nanoparticles with high anisotropic and magnetic content were obtained (Figure 8B).

By controlling the type of initiator, a spherical magnetic Janus nanoparticles; acentric of magnetics in spherical polyelectrolytes brushes consisting of PS core and poly(acrylic acid) (PAA) shell brushes were obtained via the miniemulsion polymerization using the oil soluble AIBN initiator.<sup>36</sup> The polymerization was initiated and performed inside magnetic nanoparticles (MNPs)/St monomer droplets. MNPs tended to be pushed aside of the droplet during the polymerization due to the relatively poor compatibility between PS matrix and oleic acid layer on the magnetic particle surface (Figure 9A and C).

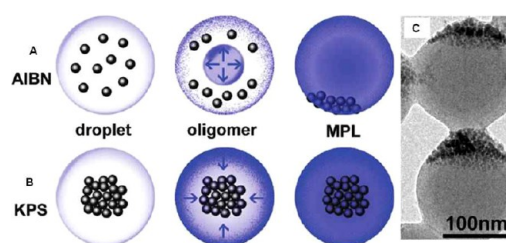


**Figure 9.** Morphology change of magnetic colloidal particles during miniemulsion polymerization using two different initiators (A) AIBN and (B) KPS. (C) TEM images of magnetic Janus colloidal nanoparticles obtained with AIBN initiator. Reproduced with permission from 36. Copyright 2011 American Chemical Society.

Compared with KPS, the polymerization initiation starts from out (water phase) to the center of the colloidal droplets, pushing MNPs to the center (core) of the droplets. Finally, magnetic colloidal particles with core-shell morphology were obtained (Figure 9B).<sup>37</sup>

The organic-inorganic Janus colloidal particles can be also synthesized by using the toposelective surface modification method. Solid surfaces, liquid/liquid, and liquid/gas interfaces have all been employed to selectively protect a part of an anisotropic particle while the exposed surface of the particle is chemically modified. The most feasible process for preparing asymmetric nanoparticles is the immobilization of the symmetric nanoparticles on solid surface. In this context, stimuli-responsive Janus beads consisting of two polymers, i.e., PAA and poly(2-vinylpyridine), grafted to the opposite sides of micrometer-sized silica particles were prepared.<sup>38</sup> Wax colloidosomes coated with amine-functionalized silica particles were exploited to selectively introduce ATRP initiator to one hemisphere using a “grafting from” approach that was used to grow polymer chains. Then, a carboxy-terminated second polymer was chemically immobilized on the opposite side of the particle, which has free amino groups, using the “grafting to” approach. The reaction between carboxyl groups of polymer chains and the amino functional groups on the particle surface led to the formation of stimulus-sensitive Janus particles to pH of the surrounding solution.

Similarly, polymer-coated magnetic Janus nanoparticles were synthesized by coating MNPs (8–10 nm) with a uniform layer of PAA brushes.<sup>39</sup> Then, a monolayer of the negatively charged PAA-coated MNPs was adsorbed onto positively charged silica



beads via electrostatic interaction. Polystyrene sodium sulfonate and/or poly(dimethylamino ethyl methacrylate) was grafted onto the exposed surface of PAA-coated MNPs by using chemical reaction. Afterward, magnetic Janus nanoparticles were recovered by increasing pH of the solution, which reversed the charge on the silica beads and repelled the adsorbed nanoparticles.

**2.4. Janus Droplets.** Recently, the microfluidic-based system has been considered as one of the most important methods used for fabrication of Janus colloidal particles. This system is based on controlling of liquids flow in microfluidic channels followed by solidification, generating monodisperse emulsions or Janus droplets.<sup>40–42</sup> The principle of this technique relies on a Y-shaped channel to form a two-phase monomer stream with a planar sheath-flow geometry. Monodisperse droplets are easily formed at the junction of the microchannels by controlling the flow rates of the dispersed and continuous phases (Figure 10A). The droplets are then

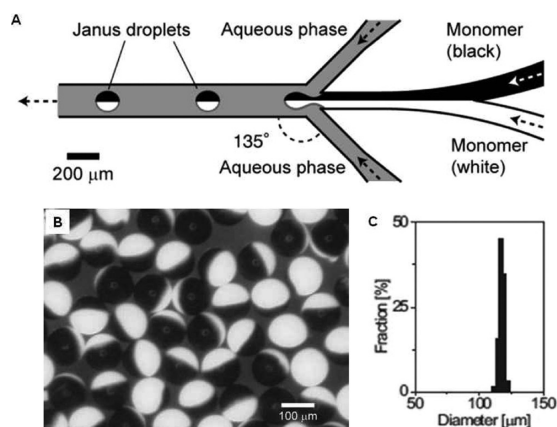


**Figure 10.** (A) Design and flow configuration of Y and sheath junctions used for the production of bicolored Janus droplets in a planar microfluidic system, (B) monodisperse bicolored Janus droplets, and (C) size distribution of the particles with mean diameter of 117  $\mu\text{m}$ . Reproduced with permission from ref 44. Copyright 2011 John Wiley and Sons.

rapidly polymerized thermally or by using UV irradiation in the outlet channel. The successful polymerization of droplets critically depends on the residence time in the irradiated region which generally decreases when increasing flow rate of the fluid. Thus, some microfluidic systems limit the in situ production of particles because of insufficient UV irradiation and incomplete polymerization, which could induce collapse or merging of Janus droplets in the out-flow channel.<sup>43</sup> Besides preparing micrometer-size Janus droplets on a large scale, the inner flow can be used to control over the location and the amount of compartments, and different components readily encapsulated in separated compartments. The electric responsive bicolor Janus particles consisted of two pigments (carbon black and titanium oxide) in different hemispherical particles were prepared by using a microfluidic coflow system (Figure 10B).<sup>44</sup> Both pigment streams were introduced into the coflow system with the same flow rate to generate bicolor emulsion droplets. The acrylic-based monomers were thermally polymerized on the outside of the microfluidic chip. Because of the difference in charge densities between carbon black and titanium oxide, the resulting Janus particles had electrical anisotropy.

Similarly, electroresponsive photonic Janus balls of silica without and with carbon-black on one side of particle dispersed in ethoxylated trimethylpropane triacrylate resin were also prepared by using the microfluidic technique.<sup>45</sup> The presence of carbon black in a half of particles could induce electrical anisotropy, which is required for electric field-induced actuation of photonic Janus ball.

Moreover, hydrogel Janus droplets can easily be prepared by using microfluidic processing technique. For instance, magnetic hydrogel Janus particles with uniform anisotropic internal structure were fabricated via flow focusing drop maker strategy using oil-in-water-in-oil (O/W/O) double emulsion droplets as template.<sup>46</sup> The droplets consisted of hydrophobic monomers (St and DVB) core with magnetic material encapsulated in hydrophilic monomers (acrylamide and N,N'-methylenebisacrylamide) droplets suspended in fluorocarbon oil. The first oil-in-water emulsion was prepared by dispersing the hydrophobic monomers with the magnetic material in an aqueous solution containing the hydrophilic monomers. Then, the obtained oil-in-water droplets flow into the second drop maker, where the wettability was inverted. This caused the water to lift off the hydrophobic interface and became encapsulated by the fluorocarbon oil phase, forming the oil-in-water-in-oil double emulsion. The Janus magnetic microgel particles with acorn-like morphology were obtained. Moreover, two magnetic cores could be encapsulated in the droplets by increasing the inner flow rate.

The microfluidic technique can be combined with bulk emulsification to fabricate Janus particles with finely tunable internal morphology. Anisotropic microgel Janus particles of polyacrylamide (PAAm) and poly(N-isopropylamide) (PNIPAm) microgel were fabricated by the induced phase separation of colloidal nanoparticles in droplets.<sup>47</sup> In this case, monodisperse droplets were produced by using capillary based microfluidic devices (Figure 11A). The square capillary served as a flow channel for the two individual fluid streams, while the circular capillary served as a collection tube for the emulsion droplets. The emulsion consisted of an aqueous phase containing cationic PNIPAm microgel, PAA, acrylamide, methylene bisacrylamide, and photoinitiator, whereas the continuous phase was a silicone oil containing surfactants. The continuous phase flow from one end of the square capillary tube, while the aqueous phase containing monomers flow from the other opposite side, meeting together at the orifice collection tube. Then, the aqueous phase broke into monodisperse droplets upon entering the correction tube to form monodisperse water-in-oil emulsion droplets. When the emulsion was heated, the weakly associated PNIPAm microgels shrank and aggregated on one side of the droplet under the combined influence of the high temperature and the electrostatic interactions between the ammonium ions of the microgels and the carboxyl groups of PAA (Figure 11B).

### 3. PROPERTIES OF JANUS PARTICLES

Janus colloidal particles possess interesting and unique properties related to their anisotropic structures, which broad their potential applications in various industrial areas and particularly in bionanotechnology. The most fascinating properties, including amphiphilic, optical, magnetic, and catalytic properties, are summarized below.

**3.1. Amphiphilic Surfactants.** Janus colloidal particles having amphiphilic property can serve as solid surfactants to emulsify an oil/water immiscible mixture. In the classic

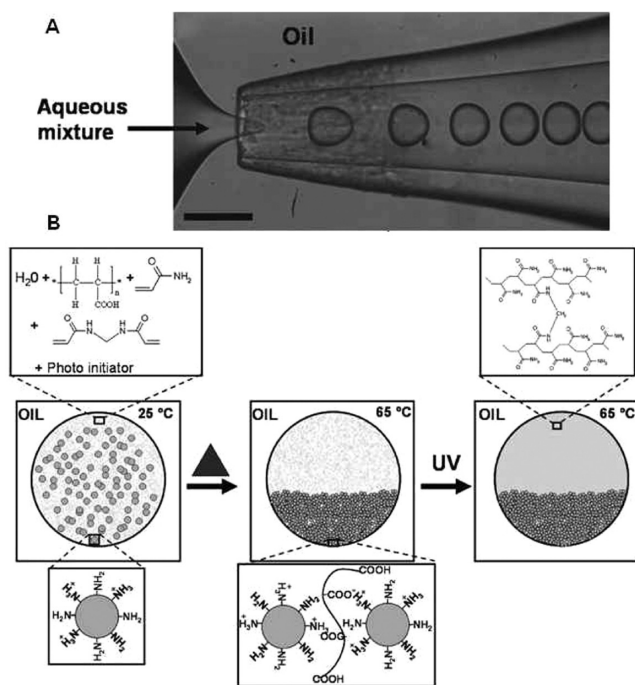


**Figure 11.** (A) Formation of monodisperse droplets in a microfluidic device with a flow focusing geometry. (B) Schematic route for the process of making Janus particles; the dispersed phase consists of an aqueous dispersion of PNIPAM microgels, PAA, and photopolymerizable monomers, whereas the continuous phase is a silicone oil containing surfactants. Upon heating, the PNIPAM microgels shrank and aggregated on one side of the droplet and acrylamide monomer was forced into the outer side of the droplets, and then polymerized and gelled using UV to form Janus gel particles. Reproduced with permission from ref 47. Copyright 2011 John Wiley and Sons.

emulsion stabilized by solid particles or Pickering emulsion, the homogeneous inorganic nanoparticles form a mechanical robust monolayer at a liquid–liquid interface to prevent the emulsion droplets against coalescence.<sup>48,49</sup> The particles are adsorbed onto the interface as a dense monolayer only under the limited conditions that depend on particle size and shape, wettability, and interparticle interaction. In contrast to a particle exhibiting uniform wettability, the surface of a Janus particles is compartmentalized and has two parts exhibiting different wettability. Therefore, a truly amphiphilic particle that combines the typical Pickering effect and the amphiphilicity of a classical surfactant can be obtained. For instance, the dumbbell-like Au–Fe<sub>3</sub>O<sub>4</sub> nanoparticles synthesized by the controlled nucleation process have been used to emulsify *n*-hexane in water.<sup>49</sup> After preparation of Au–Fe<sub>3</sub>O<sub>4</sub>, the Au part was attached by dodecanethiol (DDT) and octadecanethiol (ODT) molecules to increase the hydrophobic character of the Au part, thereby leading to an overall increase in the amphiphilic character of the particles. The presence of Janus particles (JP<sub>DDT</sub> and JP<sub>ODT</sub>) decreases the interfacial drop in the surface tension between water and *n*-hexane when compared to the homonanoparticles of Au and Fe<sub>3</sub>O<sub>4</sub> (Figure 12). Because of its nonpolar character, the hydrocarbon ligand-covered Au part oriented toward the *n*-hexane phase, and the more polar iron oxide part immersed in the aqueous phase. Similarly, the Janus particles of amphiphilic PS dimers particles exhibited stronger adsorption at the hexadecane–water interface than the isotropic particles.<sup>48</sup> Moreover, such a tendency led to jamming of the dimers particles and thus to stabilization of the

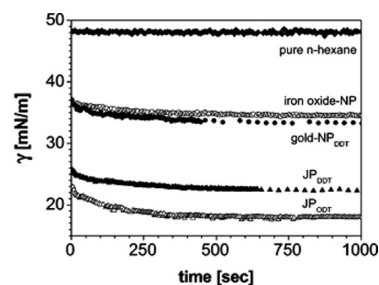


**Figure 12.** Surface activity of the nanoparticles (Interfacial tension vs time). Water was used as the drop phase, and *n*-hexane as the ambient phase in which the nanoparticles were diluted. NP is homogeneous nanoparticles, JP<sub>DDT</sub> and JP<sub>ODT</sub> are Au–Fe<sub>3</sub>O<sub>4</sub> Janus particles having Au surface modified with DDT and ODT, respectively. Reproduced with permission from ref 49. Copyright 2011 American Chemical Society.

nonspherical drops, which was not typically observed in emulsions stabilized by isotropic particles.

Janus silica/PS composite colloidal particles obtained by the seeded emulsion polymerization can also be served as solid surfactants to emulsify an oil/water immiscible mixture, which have a well-defined orientation at the oil/water interface.<sup>14</sup> After mixing Janus particles with wax-in-water emulsion at high temperature, the system was cooled to room temperature leading to the frozen orientation of Janus colloidal particles at the interface. Accordingly, the hydrophilic coarse silica part oriented toward the external aqueous phase (Figure 13) indicating that the Janus colloidal particles had a well-defined orientation at the wax/water interface.

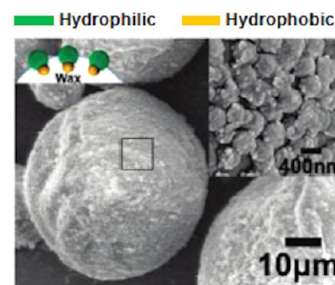


**Figure 13.** Frozen wax/water emulsion stabilized by the Janus silica/PS colloidal particles; the coarse silica side facing toward the external water phase. Reproduced with permission from ref 14. Copyright 2010 American Chemical Society.

The Janus particles incorporated with superparamagnetic nanoparticles would not only be used to stabilize emulsion but also to be easily separated from their aqueous dispersions by applying an external magnet. Similarly, the silica/PS embedded with MNPs prepared by the miniemulsion polymerization were used as emulsifier for water–toluene dual-phase system.<sup>34,35</sup> The presence of magnetic part in Janus particles is able to induce reversible macroscopic phase separation upon application of a sufficiently high external magnetic field.

**3.2. Optical and Magnetic Properties.** The incorporation of inorganic nanoparticles which possess optical or magnetic properties within Janus particle is interesting in various potential applications and particularly in the biomedical domain. The optical properties of Janus particles are dependent on the type of pigments i.e., metals (e.g., Au, CdSe and quantum dots) or fluorescent dyes (e.g., fluorescein and



rhodamine), that are embedded in the particles. The modulated optical nanoparticles (MOONs) having one side capped with metal shells, which block light transmittance, showed Brownian modulated optical property which can be exploited in bioimaging applications.<sup>50</sup> MOONs are microscopic fluorescent particles designed to emit various intensities of light in a manner that depends on particle orientation. Because of the size-dependent rotational Brownian motion, the signature frequency of fluorescence fluctuation provides a unique mechanism for identification of the MOONs. Similarly, sensing nanoprobe consisted of nanocoral structure of PS particles having Au as optically sensing nanoparticles on one side of surface and the other side containing specific ligands (anti-HER-2-antibodies) were used to detect the targeting breast cancer cells (BT474 cell line).<sup>51</sup> After incubating nanocorals with cancer cells, the phase contrast image showed nanoprobe attached to the surface of BT474 breast cancer cells. To clearly verify the location of the nanocorals on the cell surfaces, we used a fluorescent PS nanosphere. The control experiments showed that nanocorals functionalized with isotype antibodies did not attach to the cell surface.

Furthermore, Janus particles with asymmetric optical and/or magnetic properties also allow the remote control of particles movement under the effect of electrical or magnetic field. This property could be exploited and considered as a promising strategy for engineering of electronic paper and displays. For example, monodisperse bicolored Janus spheres incorporated with inorganic pigments (carbon black and titanium oxide) responsive to electric field were prepared as display materials of the electronic paper.<sup>44</sup> In the presence of an external electric field, these spheres turned to orient their black hemispheres to the negatively charged panel and vice versa. By reversing the electric field gradient, the particles flipped (Figure 14).

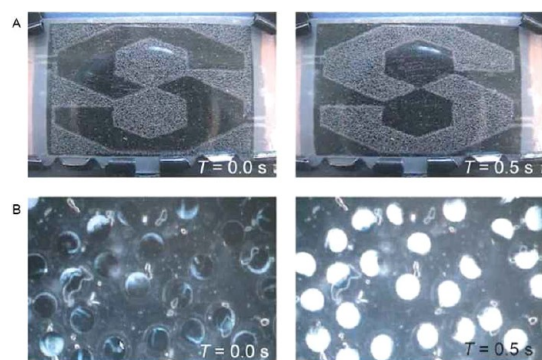


**Figure 14.** Electric actuation of the bicolored Janus particles. (A) Color switching test using prepared particles; a voltage of 100 V was applied between the 0.4 mm gap of the two electrode panels (40 mm × 40 mm) at a switching frequency of 1 Hz. (B) Magnified top view of the display panel in A. Reproduced with permission from ref 44. Copyright 2011 John Wiley and Sons.

Similarly, electroresponsive photonic Janus balls with black and structure colors regions for display application have been demonstrated.<sup>45</sup> Upon applying an alternating-current (ac) electric field through the poly(dimethylsiloxane) film, the balls began to rotate, aligning the black hemispheres along the electric field. This was attributed to the presence of carbon-black particles in one hemisphere which induced the net dipole in the Janus balls in response to the ac field.

The optical Janus particles having magnetic properties can also be controlled by an external magnetic field. For instance, bicompartamental particles with combination of two distinct hemisphere regions of quantum dots (QDs) and magnetic nanoparticles were prepared forming bifunctional magnetic-fluorescent Janus superballs.<sup>52</sup> It was found that the alternation of magnetic  $\text{Fe}_3\text{O}_4$  nanoparticles orientation depends on the direction of the applied external magnetic field; when the  $\text{Fe}_3\text{O}_4$  nanoparticle-dropped hemispheres face upward, the panel shows reddish-brown color under daylight and black color under UV light. Conversely, when the QD-polymer hemispheres orient upward, the panel displays white color under daylight and bright blue emission under UV light (Figure 15).<sup>53</sup>

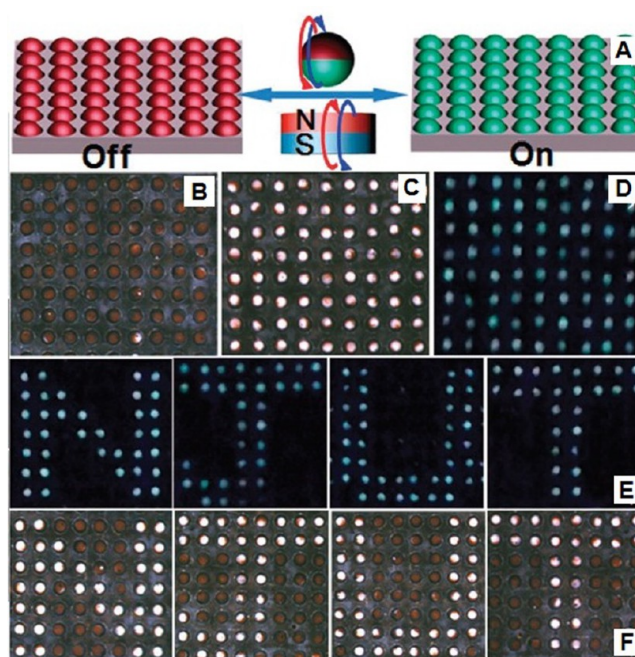


**Figure 15.** (A) Schematic representation of a fluorescent switch of Janus particles controlled by varying the direction of an external magnetic field. (B–F) Optical images of the magnetoresponsive bead display prepared from Janus particles: (B, C, F) under daylight and (D, E) under UV irradiation. Reproduced with permission from ref 53. Copyright 2011 John Wiley and Sons.

On the basis of such Janus superballs, a magnetodrive fluorescent switch would be further developed to realize free-writing under magnetic field. Moreover, magnetoresponsive Janus particles with photonic, magnetic, and structural functionalities have been demonstrated to separate particles in microfluidic pumps and mixers.<sup>53</sup> Under optical microscope, the acentric magnetic Janus particles treated with fluorescent dyes moved across to other microparticles in the mixture which responded to an applied external magnetic field.

**3.3. Catalytic Properties.** One of the potential applications of Janus particles is their use in catalysis. Metal nanoparticles dispersed on an oxide support often show a much higher catalytic activity than single-component nanoparticles. Such catalytic enhancement is attributed to the synergetic effect that occurs at the interface of metal and oxide support. It is believed that the electronic structures of both the metal and the oxide support are modified by electron transfer across the interface, giving rise to oxygen vacancies on the interfacial oxide support that becomes active sites for oxygen absorption and activation.

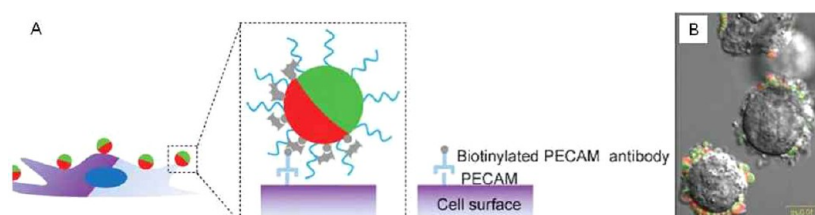


**Figure 16.** (A) Schematic representation of biocompartmental Janus particles to cells via streptavidin present on the particle surface of one compartment and biotin from cell-specific antibody (in this case PECAM). (B) Overlays of confocal laser scanning microscopy image with differential interface contrast images of self-assembly of biohybrid Janus particles and HUVECs at half cell height. Reproduced with permission from ref 58. Copyright 2009 John Wiley and Sons.

For instance, the dumbbell-like Au–Fe<sub>3</sub>O<sub>4</sub> nanoparticles showed synergetic effect in catalyzing the reduction of H<sub>2</sub>O<sub>2</sub>.<sup>54</sup> Catalytic activity of Au–Fe<sub>3</sub>O<sub>4</sub> Janus particles and of the single-components Au and Fe<sub>3</sub>O<sub>4</sub> nanoparticles which obtained by selective etching of Au–Fe<sub>3</sub>O<sub>4</sub> were studied. It was found that Au–Fe<sub>3</sub>O<sub>4</sub> nanoparticles had higher catalytic activity in H<sub>2</sub>O<sub>2</sub> reduction than Au nanoparticles, whereas H<sub>2</sub>O<sub>2</sub> reduction occurred fairly and readily on both Au–Fe<sub>3</sub>O<sub>4</sub> and the dented Fe<sub>3</sub>O<sub>4</sub> nanoparticles. Moreover, the larger size of Au nanoparticles (8 nm) in the Au–Fe<sub>3</sub>O<sub>4</sub> structure showed higher catalytic activity and stability after 100 cycles of reduction than those obtained with the small size Au (3 nm) nanoparticles because of the larger interconnection area between Au and Fe<sub>3</sub>O<sub>4</sub> nanoparticles in Au–Fe<sub>3</sub>O<sub>4</sub> structure.

Furthermore, Janus particles consisting of heterodoublets of Ag and magnetic Dynabead microspheres were demonstrated as catalytic motors in the presence of H<sub>2</sub>O<sub>2</sub> system.<sup>55</sup> The heterodoublets were fabricated via the stimulus-quench-fuse (SQF) technique with pH as the stimulus. The resulting asymmetric colloidal doublets behaved as catalytic motors showing self-propulsion and phototaxis under UV light in the presence of H<sub>2</sub>O<sub>2</sub>, by the mechanism of diffusiophoresis. The magnetic heterodoublets revealed autonomous movement, in random directions, in the presence of H<sub>2</sub>O<sub>2</sub> and UV light. However, under an external magnetic field, they aligned themselves and showed directed motion forming exclusion regions around them.

#### 4. BIOMEDICAL APPLICATIONS

Recently, the interesting properties of Janus nanoparticles have attracted attention to be used in biomedical applications such as drug delivery, molecular imaging, and bimolecular labeling. The particles with the nanometer size that can make compact Janus nanocomposites with spatially separated functionalities, uniform size, tunable composition, biocompatibility, and efficient stimuli-responsive feature are highly needed for biomedical applications.

To use Janus particles as probes in biomedical applications, the importance of local interactions between synthetic Janus particles and cell for their macroscopic functionality must be realized. Consequently, this pushed toward the synthesis of custom-tailored biohybrid materials with precisely designed physicochemical properties. In this regard, several research groups attempted to create Janus nanoparticles, so-called biohybrid materials, where cells and synthetic building blocks form structurally and functionally integrated architectures.<sup>51,56–59</sup> When designing synthesis of Janus nanoparticles for such biohybrid materials, not only the chemical makeup of bulk and interfaces have been appreciated as important design

criteria for biomaterials but also the physical properties, e.g., microstructure, anisotropic particle architecture, or shape.

Lahann et al.<sup>56–59</sup> created a novel type of microstructured hybrid biomaterials by electrohydrodynamic (EHD) cojetting of polymer-based particles with two distinct phases. The resulting anisotropic particles were used as probes for cell labeling. Then, the formed cell-particles conjugates were directly detectable; in addition cell-particle interaction was easy to investigate, as shown in Figure 16A. These anisotropic nanoparticles based on polyacrylamide/poly(acrylic acid) copolymer (P(AAm-co-AA)) exhibit different functional groups such as streptavidin on one hemisphere.<sup>58</sup> Then, after incubation period in the presence of human umbilical vein endothelial cells (HUVECs), these reactive particles were reacted with biotin-antibody specifically immobilized on targeted cell; in this case platelet endothelial cell-adhesion molecule (PECAM) was used, as shown in Figure 16B. More interestingly, these Janus nanoparticles exhibited biocompatibility with cells in addition to their nontoxicity.

In the case of drug delivery applications, Janus particles with differentially biodegradable polymer compartments were prepared for a range of oral drug delivery by using EHD technique, followed by controlled cross-linking (Figure 17).<sup>59</sup> In this regard, Janus particles composed of an interpenetrating (physical cross-linked) polymer network of poly(ethylene oxide) (PEO) and P(AAm-co-AA) in one hemisphere, and a chemically cross-linked copolymer of dextran and P(AAm-co-AA) segments in the second compartment were prepared. The compositional anisotropy of these particles caused differential hydrolytic susceptibility. Furthermore, it was found that although both compartments were stable at low pH of the stomach (i.e., pH 3), a selective degradation of the PEO-containing compartment at physiological pH (i.e., pH 7.4) was observed within 5 days. In addition, it was noted that the used cross-linking approach may not be appropriate for many drugs including protein drugs, and alternative cross-linking approaches may need to be developed in these cases. Thus, these and similar functionalized anisotropic particles are expected to find potential use for orally administrated drugs that must pass the stomach, but should release their cargo at physiological pH. Additionally, this type of multifunctional Janus particles may offer additional value because of the ability to control the pharmacokinetics of multiple drugs leading to complex release profiles.

For immunoassay applications, the heterodimer structure of the synthesized streptavidin (StAv)-functionalized protein cage can serve as a “plug and play” nanoplatform for coupling of biotinylated functional groups.<sup>60</sup> The targeting nanoplatforms were generated by assembling StAv on the surface of the nanoprotein cages (LiDps) (9 nm diameter) via toposelective



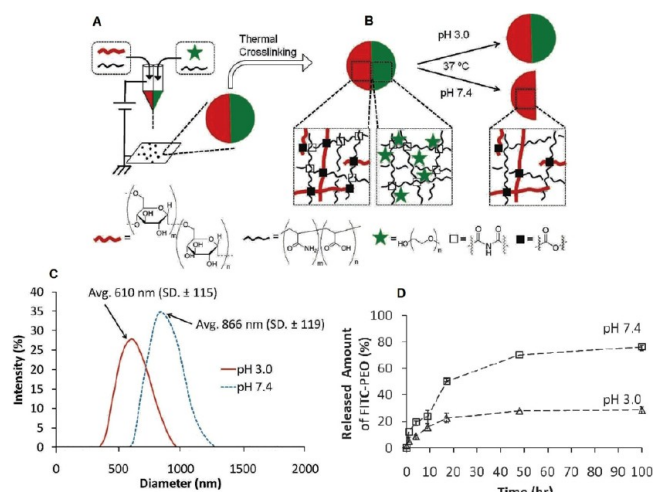


**Figure 17.** (A) Electrohydrodynamic (EHD) cojetting process used to prepare bicomparmental Janus particles based on two different polymer solutions in DI water: one solution contains poly-(acrylamide-*co*-acrylic acid) (P(AAm-*co*-AA)), dextran, and fluorescent labeled FITC-dextran, the other has P(AAm-*co*-AA) copolymer, PEO, and fluorescent labeled FITC-PEO. (B) After thermal cross-linking, two different chemical bonds (imide vs ester bonds) formed in the particle and give rise to different degradation rates for the two hemispheres. (C) Particle sizes at two different pH values (3.0 and 7.4), exhibiting that the particles are swelling at a higher pH. (D) Release profiles of FITC-PEO from the Janus particles at different pHs (pH 7.4 and pH 3.0) at 37 °C, obtained by UV spectroscopy. Reproduced with permission from ref 59. Copyright 2009 John Wiley and Sons.

modification method for fabrication of the StAv-functionalized nanoplatform. Protein cages are nanoplatforms composed of monomeric protein subunits that have been engineered to transport both diagnostic and therapeutic agents. The StAv-functionalized nanoplatforms could be used for modular functionalization with a biotinylated antibody (mAb) that specifically recognized the microbial pathogen *S. aureus* (Figure 18). The results showed that the targeting mAb can easily be

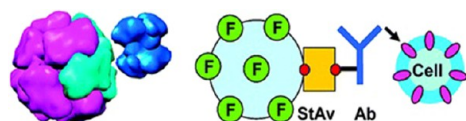


**Figure 18.** Schematic presentation for StAv-functionalized nanoplatforms coupled to a biotinylated monoclonal antibody (Ab) and used to target a microbial pathogen cell. Reproduced with permission from ref 60. Copyright 2009 American Chemical Society.

attached via the StAv-biotin couple. Besides sufficient functionalization of the heterodimer nanoplatform for targeting, many addressable sites were available for designing functional activity or cargo transport into the system.

Furthermore, Janus alginate hydrogel particles with magnetic anisotropy was prepared and used to encapsulate mammalian cells inside the hydrogel part of the magnetic alginate Janus particles to maintain optical performance, and to reduce the contact between cells and magnetic particles (Figure 19).<sup>61</sup> Alginate cell capsules prepared by this method could be easily controlled and manipulated by external magnetic fields and require no specific surface modification. In addition, the good biocompatibility, degradability and superparamagnetic proper-

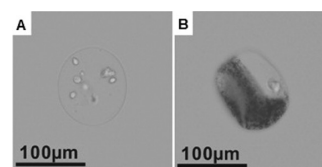


**Figure 19.** (A) Ordinary alginate hydrogel particle with mammal cells; (B) Janus hydrogel particle with mammal cells. Reproduced with permission from ref <sup>61</sup>. Copyright 2009 American Chemical Society.

ties of these Janus particles makes them suitable to be used as carriers for cells or as biochemical substances for a number of applications, such as cell culture array or targeted delivery based on magnetic control.

In diagnostic applications, Janus nanoparticles would be potentially used as probes and vectors. The enhancement of physical properties of inorganic nanoparticles arose from nanoscale phenomena. For example, dumbbell-like nanoparticles of FePt-Au having polyethylene glycol based ligands on their surfaces were used as probes for magnetic resonance imaging (MRI) of tumor cell targets.<sup>20</sup> The FePt-Au heterodimers obtained by the controlled nucleation method were conjugated with HmenB1 antibodies which specifically recognized polysialic acid (PSA). The PSA is an important carbohydrate associated with tumor cell growth and metastasis. The FePt-Au/HmenB1 conjugate nanoparticles were tested on two different cell lines: target cells (CHP-134) with over-expression of PSA and control cells (HEK293T) without PSA. In the T<sub>s</sub>\* gradient echo images at 9.4T, although no MRI contrast was observed from the PSA negative control cells, the MRI contrast effect with significant increase of ~133% in R<sub>2</sub>\* relaxivity (= 1/T<sub>2</sub>\*) was clearly seen from the FePt-Au/HmenB1 conjugate nanoparticles treated PSA positive cells.

Moreover, Janus nanoparticles with optical and magnetic properties can be used in high potential diagnostic and therapeutic applications. For example, the spherical Janus nanoparticles of magnetic nanoparticles/pyrene label poly-(styrene-block-allyl alcohol) were obtained based on the controlled phase separation for use in both imaging and treatment of cancer cells (Figure 20A).<sup>62</sup> On the basis of

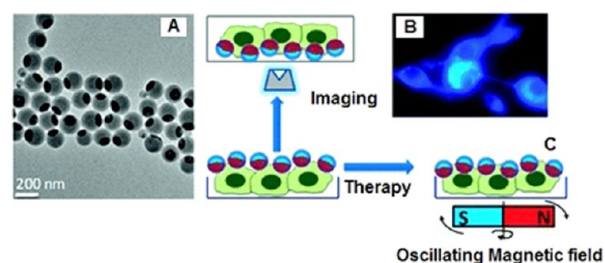


**Figure 20.** (A) TEM of Janus nanocomposites with spatially separated functionalities for (B) combined fluorescence imaging and for (C) magnetolytic therapy of cancer cells. Reproduced with permission from ref 62. Copyright 2010 American Chemical Society.

magnetic modulation (the orientation strategy for cell imaging application), cell particle attachment was achieved through the nonspecific adsorption facilitated by magnetic manipulation which clearly observed by fluorescence microscopy (Figure 20B). For investigation of therapeutic effect of the particles, cells were placed in a spinning magnetic field (50 rpm), which generated a mechanical force on the cell membrane (Figure



20C). After 15 min of exposure to the spinning magnetic field, the majority of the tumor cells were killed and identified by Trypan blue staining. The number of live cells after magnetolytic therapy compared with the control was reduced by 77%, whereas those missing either nanocomposites or magnetic fields showed >99.5% cell survival.

Similarly, live macrophage cells bound to Janus nanoparticles of silver/magnetite ( $\text{Ag}/\text{Fe}_3\text{O}_4$ ) have been manipulated by external magnetic field and imaged.<sup>23</sup> However, the selective surface functionalization plays a critical role in imaging probe and for novel simultaneous targeting capabilities, complex drug release profiles, and smart imaging competence. Moreover, dumbbell-like gold/magnetite ( $\text{Au}/\text{Fe}_3\text{O}_4$ ) nanoparticles served as a multifunctional platform for target-specific platin delivery into Her2-positive breast cancer cells.<sup>63</sup> The presence of two different nanoparticle surfaces within one nanostructure facilitated the controlled functionalization of each particle. Their core structure contained MNPs and optically Au nanoparticles (Figure 21). The platin complex was anchored

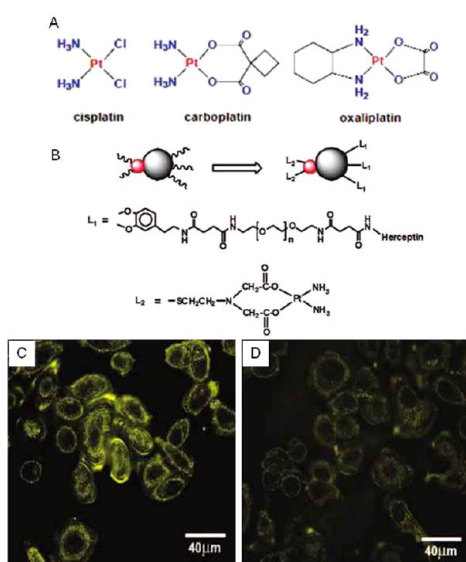


**Figure 21.** (A) Structures of the common therapeutic platin complexes, (B) schematic presentation of the dumbbell-like  $\text{Au}/\text{Fe}_3\text{O}_4$  nanoparticles coupled with Herceptin and a platin complex for target-specific platin delivery, and reflection images of (C) Sk-Br3 and (D) MCF-7 control cells after incubation with the same concentration of platin  $\text{Au}/\text{Fe}_3\text{O}_4$  nanoparticles. Reproduced with permission from ref.<sup>63</sup>. Copyright 2010 American Chemical Society.

on the Au side and the Her2-specific monoclonal antibody Herceptin chosen as a targeting agent was linked to  $\text{Fe}_3\text{O}_4$ . The release of the therapeutic platin under low-pH conditions allowed the nanoparticles to conjugate and to be more toxic to the targeted tumor cells (Sk-Br3 cell) than free cisplatin. The target-specific delivery through strong antibody–antigen interactions and receptor-mediated endocytosis were achieved.

Similar to silver/magnetite ( $\text{Ag}/\gamma\text{-Fe}_2\text{O}_3$ ), Janus nanoparticles coated with silica can be utilized as biocompatible cellular biomarkers.<sup>64</sup> Their performance as biomarkers was explored by selectively binding them with live tagged Raji and HeLa cells enabling both detection and magnetic recovery. The Janus nanoparticles of  $\text{Ag}/\gamma\text{-Fe}_2\text{O}_3$  coated with silica prevented the individual limitations of  $\gamma\text{-Fe}_2\text{O}_3$  (poor particle stability in suspensions) and Ag (toxicity) nanoparticles, retaining at the same time the desired magnetic properties of  $\gamma\text{-Fe}_2\text{O}_3$ , the inert

surface of silica, and the plasmonic optical properties of Ag at the nanoscale.

## 5. CONCLUSIONS AND REMARKS

Colloidal particles with Janus morphology are composed of at least two opposite parts with various structural/physical and/or chemical properties which can be exploited in various potential industrial (e.g., emulsion stabilization, electronic paper, photonic materials, and catalysis) and biomedical applications. In the biomedical field, the feasibility of controlling the asymmetric structure of Janus nanoparticles allows to enhance multifunctionality which maximizes the efficacy of drug-, gene-, and immunotherapy. In addition, they can be used in molecular imaging as biomarkers or as optical probes.

Recently, various synthetic approaches mainly based on the phase separation and the topospecific surface modification strategies have been used for preparing Janus colloidal particles. The most commonly used synthetic approaches include polymerization in dispersed media (e.g., emulsion, miniemulsion and double emulsion polymerization), fabrication through microfluidic devices, and topospecific surface modification method. Each method shows various advantages and some limitations in the fabrication of Janus colloidal particles for specific applications. For example, microfluidic devices can be used to produce large amount of Janus droplets particles in a continuous fashion. However, the relatively large size of fluidic channels leads to larger size particles. Therefore, the sizes of the prepared colloidal particles range from one to hundreds of micrometers, which is not convenient to apply in some biomedical applications. In addition, the components are greatly restricted, and the solid content is rather low. On the other hand, topospecific surface modification requires several steps for preparation of template particles and/or temporary masking of one hemisphere, surface modification of the other half, and for liberation of Janus particles.

As a final conclusion, the preparation of Janus colloidal particles is still a significant challenge which considered as the key point for extending their use in more specific fields, particularly in the biomedicine.

## AUTHOR INFORMATION

### Corresponding Author

\*E-mail: elaissari@lagep.univ-lyon1.fr.

### Present Address

<sup>1</sup>M.E. is currently at Polymers and Pigments Department, National Research Centre, Dokki, Giza 12622, Egypt

### Notes

The authors declare no competing financial interest.

## ACKNOWLEDGMENTS

The authors appreciate the research grant (RTA5480007) from The Thailand Research Fund (TRF)/Commission on Higher Education to P.T., and the scholarship from TRF, Mahidol University and French Government through the Royal Golden Jubilee Ph.D. Program (Grant PHD/0174/2552) to PhD student C.K. All facilities supported by Laboratory of Automatic Control and Processing Engineering, LAGEP laboratory, Claude Bernard University, UMR-5007, CPE-Lyon, are gratefully acknowledged.

## ■ REFERENCES

- (1) Poletto, F. S.; Fiel, L. A.; Lopes, M. V.; Schaab, G.; Gomes, A. M. O.; Guterres, S. S.; Rossi-Bergmann, B.; Pohlmann, A. R. *J. Colloid Sci. Biotechnol.* **2012**, *1*, 89–98.
- (2) Ahmed, N.; Jamois, M. M.; Fessi, H.; Elaissari, A. *Soft Matter* **2012**, *8*, 2554–2564.
- (3) Rahman, M. M.; Elaissari, A. *J. Colloid Sci. Biotechnol.* **2012**, *1*, 3–15.
- (4) Eissa, M. M.; Rahman, M. M.; Zine, N.; Jaffrezic, N.; Errachid, A.; Fessi, H.; Elaissari, A. *Acta Biomater.* **2013**, *9*, 5573–5582.
- (5) Roveimiab, Z.; Mahdavian, A. R.; Biazar, E.; Heidari, K. S. *J. Colloid Sci. Biotechnol.* **2012**, *1*, 82–88.
- (6) Wurm, F.; Kilbinger, A. F. M. *Angew. Chem., Int. Ed.* **2009**, *48*, 8412–8421.
- (7) Jiang, S.; Chen, Q.; Tripathy, M.; Luijten, E.; Schweizer, K. S.; Granick, S. *Adv. Mater.* **2010**, *22*, 1060–1071.
- (8) Cho, I.; Lee, K. W. *J. Appl. Polym. Sci.* **1985**, *30*, 1903–1926.
- (9) de Gennes, P. G. *Rev. Mod. Phys.* **1992**, *64*, 645–648.
- (10) Hu, J.; Zhou, S.; Sun, Y.; Fang, X.; Wu, L. *Chem. Soc. Rev.* **2012**, *41*, 4356–4378.
- (11) Yang, S.-M.; Kim, S.-H.; Lim, J.-M.; Yi, G.-R. *J. Mater. Chem.* **2008**, *18*, 2177–2190.
- (12) Yoon, J.; Lee, K. J.; Lahann, J. *J. Mater. Chem.* **2011**, *21*, 8502–8510.
- (13) Lattuada, M.; Hatton, T. A. *Nano Today* **2011**, *6*, 286–308.
- (14) Tang, C.; Zhang, C.; Liu, J.; Qu, X.; Li, J.; Yang, Z. *Macromolecules* **2010**, *43*, 5114–5120.
- (15) Pfau, A.; Sander, R.; Kirsch, S. *Langmuir* **2002**, *18*, 2880–2887.
- (16) Wang, Y.; Guo, B.-H.; Wan, X.; Xu, J.; Wang, X.; Zhang, Y.-P. *Polymer* **2009**, *50*, 3361–3369.
- (17) Tanaka, T.; Okayama, M.; Kitayama, Y.; Kagawa, Y.; Okubo, M. *Langmuir* **2010**, *26*, 7843–7847.
- (18) Ahmad, H.; Saito, N.; Kagawa, Y.; Okubo, M. *Langmuir* **2008**, *24*, 688–691.
- (19) Perro, A.; Reculosa, S.; Ravaine, S.; Bourgeat-Lami, E.; Duguet, E. *J. Mater. Chem.* **2005**, *15*, 3745–3760.
- (20) Choi, J.-S.; Jun, Y.-W.; Yeon, S. I.; Kim, H. C.; Shin, J.-S.; Cheon, J. *J. Am. Chem. Soc.* **2006**, *128*, 15982–15983.
- (21) Lu, Y.; Xiong, H.; Jiang, X.; Xia, Y. *J. Am. Chem. Soc.* **2003**, *125*, 12724–12725.
- (22) Yu, H.; Chen, M.; Rice, P. M.; Wang, S. X.; White, R. L.; Sun, S. *Nano Lett.* **2005**, *5*, 379–382.
- (23) Jiang, J.; Gu, H.; Shao, H.; Devlin, E.; Papaefthymiou, G. C.; Ying, J. Y. *Adv. Mater.* **2008**, *20*, 4403–4407.
- (24) Lin, C.-C.; Liao, C.-W.; Chao, Y.-C.; Kuo, C. *ACS Appl. Mater. Interfaces* **2010**, *2*, 3185–3191.
- (25) Ling, X. Y.; Phang, I. Y.; Acikgoz, C.; Yilmaz, M. D.; Hempenius, M. A.; Vancso, G. J.; Huskens, J. *Angew. Chem., Int. Ed.* **2009**, *48*, 7677–7682.
- (26) Braconnot, S.; Eissa, M. M.; Elaissari, A. *Colloid Polym. Sci.* **2013**, *291*, 193–203.
- (27) Montagne, F.; Mondain-Monval, O.; Pichot, C.; Elaissari, A. *J. Polym. Sci. A: Polym. Chem.* **2006**, *44*, 2642–2656.
- (28) Rahman, M. M.; Montagne, F.; Fessi, H.; Elaissari, A. *Soft Matter* **2011**, *7*, 1483–1490.
- (29) Ge, J.; Hu, Y.; Zhang, T.; Yin, Y. *J. Am. Chem. Soc.* **2007**, *129*, 8974–8975.
- (30) Reculosa, S.; Poncet-Legrand, C.; Perro, A.; Duguet, E.; Bourgeat-Lami, E.; Mingotaud, C.; Ravaine, S. *Chem. Mater.* **2005**, *17*, 3338–3344.
- (31) Qiang, W.; Wang, Y.; He, P.; Xu, H.; Gu, H.; Shi, D. *Langmuir* **2008**, *24*, 606–608.
- (32) Ge, X.; Wang, M.; Yuan, Q.; Wang, H.; Ge, X. *Chem. Commun.* **2009**, 2765–2767, DOI: 10.1039/B901094G.
- (33) Lu, W.; Chen, M.; Wu, L. *J. Colloid Interface Sci.* **2008**, *328*, 98–102.
- (34) Teo, B. M.; Suh, S. K.; Hatton, T. A.; Ashokkumar, M.; Grieser, F. *Langmuir* **2011**, *27*, 30–33.
- (35) Wang, Y.; Xu, H.; Ma, Y.; Guo, F.; Wang, F.; Shi, D. *Langmuir* **2011**, *27*, 7207–7212.
- (36) Chen, K.; Zhu, Y.; Zhang, Y.; Li, L.; Lu, Y.; Guo, X. *Macromolecules* **2011**, *44*, 632–639.
- (37) Mori, Y.; Kawaguchi, H. *Colloids Surf., B* **2007**, *56*, 246–254.
- (38) Berger, S.; Synytska, A.; Ionov, L.; Eichhorn, K.-J.; Stamm, M. *Macromolecules* **2008**, *41*, 9669–9676.
- (39) Lattuada, M.; Hatton, T. A. *J. Am. Chem. Soc.* **2007**, *129*, 12878–12889.
- (40) Teh, S.-Y.; Lin, R.; Hung, L.-H.; Lee, A. P. *Lab Chip* **2008**, *8*, 198–220.
- (41) Yang, S.; Guo, F.; Kiraly, B.; Mao, X.; Lu, M.; Leong, K. W.; Huang, T. J. *Lab Chip* **2012**, *12*, 2097–2102.
- (42) Serra, C. A.; Chang, Z. *Chem. Eng. Technol.* **2008**, *31*, 1099–1115.
- (43) Prasad, N.; Perumal, J.; Choi, C.-H.; Lee, C.-S.; Kim, D.-P. *Adv. Funct. Mater.* **2009**, *19*, 1656–1662.
- (44) Nisisako, T.; Torii, T.; Takahashi, T.; Takizawa, Y. *Adv. Mater.* **2006**, *18*, 1152–1156.
- (45) Kim, S.-H.; Jeon, S.-J.; Jeong, W. C.; Park, H. S.; Yang, S.-M. *Adv. Mater.* **2008**, *20*, 4129–4134.
- (46) Chen, C.-H.; Abate, A. R.; Lee, D.; Terentjev, E. M.; Weitz, D. A. *Adv. Mater.* **2009**, *21*, 3201–3204.
- (47) Shah, R. K.; Kim, J.-W.; Weitz, D. A. *Adv. Mater.* **2009**, *21*, 1949–1953.
- (48) Kim, J.-W.; Lee, D.; Shum, H. C.; Weitz, D. A. *Adv. Mater.* **2008**, *20*, 3239–3243.
- (49) Glaser, N.; Adams, D. J.; Boker, A.; Krausch, G. *Langmuir* **2006**, *22*, 5227–5229.
- (50) Behrend, C. J.; Anker, J. N.; McNaughton, B. H.; Brasuel, M.; Philibert, M. A.; Kopelman, R. *J. Phys. Chem. B* **2004**, *108*, 10408–10414.
- (51) Wu, L. Y.; Ross, B. M.; Hong, S.; Lee, L. P. *Small* **2010**, *6*, 503–507.
- (52) Yin, S.-N.; Wang, C.-F.; Yu, Z.-Y.; Wang, J.; Liu, S.-S.; Chen, S. *Adv. Mater.* **2011**, *23*, 2915–2919.
- (53) Kim, S.-H.; Sim, J. Y.; Lim, J.-M.; Yang, S.-M. *Angew. Chem., Int. Ed.* **2010**, *49*, 3786–3790.
- (54) Lee, Y.; Garcia, M. A.; Frey Huls, N. A.; Sun, S. *Angew. Chem., Int. Ed.* **2010**, *49*, 1271–1274.
- (55) Chaturvedi, N.; Hong, Y.; Sen, A.; Velegol, D. *Langmuir* **2010**, *26*, 6308–6313.
- (56) Roh, K.-H.; Matrin, D. C.; Lahann, J. *Nat. Mater.* **2005**, *4*, 759–763.
- (57) Yoshida, M.; Roh, K.-H.; Lahann, J. *Biomaterials* **2007**, *28*, 2446–2456.
- (58) Yoshida, M.; Roh, K.-H.; Mandal, S.; Bhaskar, S.; Lim, D.; Nandivada, H.; Deng, X.; Lahann, J. *Adv. Mater.* **2009**, *21*, 4920–4925.
- (59) Hwang, S.; Lahann, J. *Macromol. Rapid Commun.* **2012**, *33*, 1178–1183.
- (60) Suci, P. A.; Kang, S.; Young, M.; Douglas, T. *J. Am. Chem. Soc.* **2009**, *131*, 9164–9165.
- (61) Zhao, L. B.; Pan, L.; Zhang, K.; Guo, S. S.; Liu, W.; Wang, Y.; Chen, Y.; Zhao, X. Z.; Chan, H. L. W. *Lab Chip* **2009**, *9*, 2981–2986.
- (62) Hu, S.-H.; Gao, X. *J. Am. Chem. Soc.* **2010**, *132*, 7234–7237.
- (63) Xu, C.; Wang, B.; Sun, S. *J. Am. Chem. Soc.* **2009**, *131*, 4216–4217.
- (64) Soyirliou, G. A.; Hirt, A. M.; Lozach, P.-Y.; Teleki, A.; Krumeich, F.; Pratsinis, S. E. *Chem. Mater.* **2011**, *23*, 1985–1992.